Higher-order glass-transition singularities in systems with short-ranged attractive potentials



2003 J. Phys.: Condens. Matter 15 S869

(http://iopscience.iop.org/0953-8984/15/11/311)

INSTITUTE OF PHYSICS PUBLISHING JOURNAL OF PHYSICS: CONDENSED MATTER

J. Phys.: Condens. Matter **15** (2003) S869–S879 PII: S0953-8984(03)58107-3

# Higher-order glass-transition singularities in systems with short-ranged attractive potentials

**W Götze and M Sperl**

Physik-Department, Technische Universität München, 85747 Garching, Germany

Received 27 September 2002
Published 10 March 2003
Online at stacks.iop.org/JPhysCM/15/S869

**Abstract**

Within the mode-coupling theory for the evolution of structural relaxation, the $A_4$-glass-transition singularities are identified for systems of particles interacting with a hard-sphere repulsion complemented by different short-ranged potentials: Baxter's singular potential regularized by a large-wavevector cut-off, a model for the Asakura–Oosawa depletion attraction, a triangular potential, a Yukawa attraction, and a square-well potential. The regular potentials yield critical packing fractions, critical Debye–Waller factors, and critical amplitudes very close to each other. The elastic moduli and the particle localization lengths for corresponding states of the Yukawa system and the square-well system may differ by up to 20 and 10%, respectively.

## 1. Introduction

In this paper, some results will be presented for the liquid–glass transition diagrams of simple systems as obtained within mode-coupling theory (MCT) [1] for the evolution of structural relaxation. This theory is based on closed non-linear equations of motion for the normalized autocorrelation functions for density fluctuations with wavevector modulus $q = |\vec{q}|$, $\phi_q(t)$. Liquid states are characterized by solutions vanishing for large times $t$, $\phi_q(t \to \infty) = 0$. Glasses are characterized by solutions whose long-time limits are the non-vanishing Debye–Waller factors of the arrested amorphous structure $f_q = \phi_q(t \to \infty)$, $0 < f_q \leqslant 1$. The $f_q$ obey the set of implicit equations

$$\frac{f_q}{1 - f_q} = \mathcal{F}_q[f_k]. \tag{1a}$$

The mode-coupling functional $\mathcal{F}_q$ reads

$$\mathcal{F}_q[f_k] = \sum_{\vec{k}+\vec{p}=\vec{q}} V(\vec{q}, \vec{k}, \vec{p}) f_k f_p \tag{1b}$$

with coupling coefficients

$$V(\vec{q}, \vec{k}, \vec{p}) = \rho S_q S_k S_p \{[\vec{k} c_k + \vec{p} c_p] \cdot \vec{q}/q\}^2/(2q^2). \tag{2}$$

0953-8984/03/110869+11$30.00  

Here, $S_q$ and $c_q$ are the structure factor and the direct correlation function, respectively, related by the Ornstein–Zernicke equation $S_q = 1/[1 - \rho c_q]$. The structure factor depends on control parameters such as the particle density $\rho$, the temperature $T$, and parameters specifying the dependence of the interaction potential $U(r)$ on the interparticle distance $r$. Let us combine the set of control parameters considered to a control-parameter vector $\boldsymbol{V}$. The discussion will be restricted to parameter regions where $S_q$, and hence $\mathcal{F}_q$, depend smoothly on $\boldsymbol{V}$. The Debye–Waller factor $f_q$ for a given $\boldsymbol{V}$ is distinguished from other possible solutions of equations (1) and (2), for the same $\boldsymbol{V}$, say $\tilde{f}_q$, by the maximum property: $f_q \geqslant \tilde{f}_q$ for all $q$.

For almost all control parameters, the Debye–Waller factors $f_q$ depend smoothly on $\boldsymbol{V}$. The exceptional points are referred to as glass-transition singularities $\boldsymbol{V}^{\mathrm{c}}$. These critical points of equations (1) and (2) are bifurcation singularities of the cuspoid family $A_l, l = 2, 3, \ldots$. An $A_l$-bifurcation describes a topologically stable singularity that is equivalent to the bifurcation singularities of the zeros of a real polynomial of degree $l$ [2]. The liquid–glass transition points are $A_2$-singularities located on smooth surfaces in parameter space. If $\boldsymbol{V}$ crosses this surface at some $\boldsymbol{V}^{\mathrm{c}}$, the long-time limit $\phi_q(t \to \infty)$ jumps from zero to the critical Debye–Waller factor $f_q^{\mathrm{c}} > 0$. There may exist surfaces of $A_2$-singularities within the glass. These describe iso-structural transitions from one amorphous state characterized by $f_q > 0$ to another state specified by a larger Debye–Waller factor $f_q^{\mathrm{c}} > f_q$. For every $A_2$-singularity, a number $\lambda$, $0.5 \leqslant \lambda < 1$, can be calculated. It is called the exponent parameter since it determines the various anomalous exponents entering the description of the slow dynamics for $\boldsymbol{V}$ near $\boldsymbol{V}^{\mathrm{c}}$. The higher-order singularities, $A_l$, $l \geqslant 3$, are the end-points of the transition surfaces characterized by $\lambda = 1$. In the following, some properties of $A_4$-singularities $\boldsymbol{V}^*$ will be discussed. Interparticle interactions will be considered, consisting of a hard-sphere repulsion core of diameter $d$ and a short-ranged attraction potential for $r > d$. The latter will be parametrized by a typical attraction strength $u_0$ and a typical attraction range $\Delta$. Therefore, a three-dimensional control-parameter space is considered: $\boldsymbol{V} = (\varphi, \Gamma, \delta)$, where $\varphi = (\pi/6)\rho d^3$ denotes the packing fraction of the spheres, $\Gamma = u_0/(k_{\mathrm{B}}T)$ is a dimensionless attraction strength or an inverse dimensionless temperature, and $\delta = \Delta/d$ is an attraction-range parameter.

For a system of particles interacting with a hard-sphere repulsion complemented by a short-ranged attraction, MCT leads to two intriguing results [3, 4]. First, the increase of the attraction strength $\Gamma$ may cause a melting of the glass. This implies a re-entry phenomenon for the transition diagram. For certain values of the packing fraction $\varphi$, the liquid freezes into a glass not only on cooling but also on heating. This prediction has been verified recently for colloidal suspensions [5, 6]. In this work, the parameter $\Gamma$ was varied by adding polymer to the solvent, thereby increasing the strength of the depletion attraction. The re-entry phenomenon was also established by molecular dynamics simulation studies [5, 7–9]. Second, the existence of an $A_3$-singularity was predicted. The glass–glass transitions connected with this higher-order singularity deal with discontinuous changes of the localization mechanism from one caused by the repulsion-induced cage effect to one caused by the attraction-induced bonding of the particles. The cited work was based on Baxter's model for sticky hard spheres (SHS) [10] complemented with a large-cut-off wavevector $q_{\mathrm{co}}$ restricting the wavevector sums in the mode-coupling functional from equation (1$b$). The effective range of the regularized potential introduced by the cut-off can be parametrized by $\Delta = \pi/q_{\mathrm{co}}$. The singular Baxter interaction leads to a large-$q$ tail for the direct correlation function $c_q = \mathcal{O}(1/q)$. It is this tail for $2\pi/d < q < q_{\mathrm{co}}$ that causes the $A_3$-bifurcation. This $A_3$-singularity disappears if $q_{\mathrm{co}}$ is decreased towards $2\pi/d$.

The generic scenario for the disappearance of an $A_3$-singularity in a three-parameter system is the existence of an $A_4$-glass-transition singularity at some point $\boldsymbol{V}^* = (\varphi^*, \Gamma^*, \delta^*)$.

Thus, the cited results [1–4] lead to the following conclusion. A system of particles interacting with some steep strong repulsion core complemented by a sufficiently strong short-ranged attraction potential exhibits an $A_4$-singularity at some control-parameter point $\boldsymbol{V}^*$. The general transition diagram is organized around this $\boldsymbol{V}^*$. Diagrams for different models for the interparticle interaction can be mapped onto each other for small $\boldsymbol{V}-\boldsymbol{V}^*$ by a smooth invertible parameter transformation. In this sense, the bifurcation scenario is universal. The scenario at an $A_4$-singularity has been shown in some detail for the square-well system (SWS) [11]. In the following, these results will be extended and compared with the ones calculated for other potentials that might be of interest for the description of colloidal systems.

## 2. Results

Let us specify the attraction potentials to be considered and the approximation theories to be used to evaluate $S_q$. The model of SHS complemented by the above-mentioned cut-off $q_{\mathrm{co}}$ will be used with the convention $\Gamma = 15/\tau$. For the definition of the stickiness parameter $\tau$ and the evaluation of the structure factor, we follow Baxter's work [10]. The hard-core Yukawa system (HCY) is used with the following convention for the control parameters:

$$U(r)/(k_{\mathrm{B}}T) = -\Gamma \exp[-(r-d)/(\delta d)]/(r/d), \qquad d < r, \tag{3}$$

i.e., $\delta$ is chosen as the inverse of the conventional screening parameter $b$. The structure factor is evaluated analytically in the mean-spherical approximation [12]. Furthermore, three potentials of polynomial shape are considered:

$$U(r)/(k_{\mathrm{B}}T) = -\Gamma[(d+\delta d-r)/(\delta d)]^{(n-1)}, \qquad d < r < (1+\delta)d. \tag{4}$$

For $n = 1$, the formula describes the SWS. The triangular-potential model (TRI) is obtained for $n = 2$. The Asakura–Oosawa system (AOS) is modelled by $n = 3$. The latter potential is obtained as the small-$\delta$ limit for the depletion attraction acting between spheres in a dilute solvent of small polymers [13]. It was shown that the equations for the mean-spherical approximation for $S_q$ of the SWS can be solved analytically by an expansion in $\delta$ [11]. This procedure can be extended to treat the potentials of equation (4) for every $n$. The leading-order expansion formulae are given in the appendix, and they are used in the following. Let us recall that for the range of length parameters of interest, say $\delta < 0.20$ for the SWS, the next-to-leading-order result is very close to the full numerical solution for $n = 1$ [11].

To determine $f_q$ for a given $\boldsymbol{V}$, the standard iteration procedure is applied: $f_q^{(n)}/(1-f_q^{(n)}) = \mathcal{F}_q[f_k^{(n-1)}]$, $n = 1, 2, \ldots$, $f_q^{(0)} = 1$, $\lim_{n\to\infty} f_q^{(n)} = f_q$ [1]. This is done after equations (1) and (2) have been rewritten so that the wavevector moduli are discretized to $M$ points on a grid of equal spacing $h$. The values $h = 0.4/d$ and $M = 300$ have been used to identify the $A_2$-singularities on the bifurcation surface. It is onerous to identify the higher-order singularities, since $(l-1)$ control parameters have to be scanned and the convergence of the iteration is slower for points at an $A_{l+1}$-singularity than at an $A_l$-singularity. One can use the deviation of $\lambda$ from unity to characterize the error for the identification of an $A_l$ with $l \geqslant 3$. In our calculations we achieved $1-\lambda < 10^{-3}$. At the end, the calculation at $\boldsymbol{V}^*$ was repeated with $h = 0.08/d$ and $M = 1500$ in order to check the independence of the results of the discretization approximation.

As a representative example, figure 1 exhibits the glass-transition-singularity diagram of the HCY. The inner points of the lines are $A_2$-singularities obtained as constant-$\delta$ cuts through the bifurcation manifold in the three-dimensional space of control parameters $\boldsymbol{V}$. There are three topologically different cuts. The smooth curve shown for $\delta = 0.0250$ represents a typical cut for $\delta > \delta^*$. All points describe liquid–glass transitions characterized by an exponent

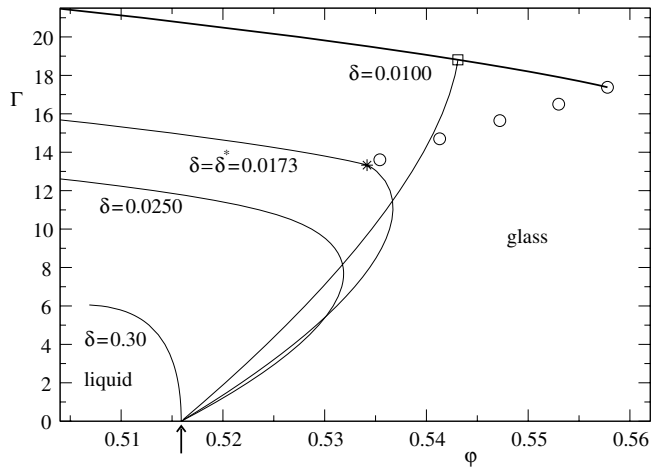


**Figure 1.** The transition diagram for the HCY. The attraction strength $\Gamma$ versus packing fraction $\varphi$ curves show cuts through the surfaces of glass-transition singularities for fixed attraction-range parameter $\delta$ as indicated; cf equation (3). The curve for $\delta = \delta^* = 0.0173$ hits the $A_4$-singularity ($*$). The line for $\delta = 0.0100$ exhibits a crossing point ($\square$), and an $A_3$-singularity ($\bigcirc$). Four further $A_3$-singularities are marked by circles; they refer from left to right to $\delta = 0.0167, 0.0143, 0.0125, 0.0111$. The arrow points to the critical packing fraction $\varphi^{\rm c}_{\rm HSS} = 0.516$ for the HSS.

parameter $\lambda < 1$. For $\delta = \delta^* = 0.0173\ldots$, the transition curve runs through the $A_4$-singularity marked by a star. For all $\boldsymbol{V} \neq \boldsymbol{V}^*$, the curve is smooth and $\lambda < 1$. For $\boldsymbol{V} = \boldsymbol{V}^*$, $\lambda = 1$ and the curve has a continuous tangent but an infinite curvature. The curves for $\delta < \delta^*$ each consist of two pieces as demonstrated for $\delta = 0.0100$. The part shown as a heavy curve with $\mathrm{d}\Gamma^{\rm c}/\mathrm{d}\varphi^{\rm c} < 0$ terminates within the glass in an $A_3$-singularity marked by a circle. The second part shown as a light curve terminates in a crossing point indicated by a square. The curve of $A_2$-singularities between the crossing point and the $A_3$-singularity deals with glass–glass transitions and the other part with liquid–glass transitions. $A_2$-glass-transition curves for the HCY for $\delta \neq \delta^*$ cuts have been considered previously for the HCY [4, 14, 15].

Let us add a remark on the diagram. Obviously, for $\Gamma = 0$, all cuts start at the critical packing fraction of the hard-sphere system (HSS), $\varphi^{\rm c}_{\rm HSS} = 0.516$. There is a characteristic range parameter $\delta_{\rm re-entry}$: the slope $\mathrm{d}\Gamma^{\rm c}/\mathrm{d}\varphi^{\rm c}$ for $\Gamma = 0$ is negative for $\delta > \delta_{\rm re-entry}$ and positive for $\delta < \delta_{\rm re-entry}$. The latter case is exemplified in figure 1 by the three cuts discussed in the preceding paragraph; the former case is shown by the cut for $\delta = 0.300$. For $\delta < \delta_{\rm re-entry}$ and sufficiently small $\Gamma$, the transition curves deal with melting of the glass upon increasing the attraction parameter $\Gamma$. Hence, for all liquid states with $\varphi > \varphi^{\rm c}_{\rm HSS}$, one gets the re-entry phenomenon mentioned in the introduction. The bonding forces create holes in the cages and this can destroy the particle localization for long times. In agreement with Lindemann's melting criterion, the critical localization length of the HSS is about $r^{\rm c}_{\rm s} = 0.0746d$. If the attraction potential range $\Delta$ is much larger than $r^{\rm c}_{\rm s}$, i.e., if $\delta$ exceeds a critical value $\delta_{\rm re-entry}$, the bonding effects cannot change the cage structure. Therefore, the re-entry mechanism disappears for $\delta > \delta_{\rm re-entry}$. In this case, the transition curve is similar to the one obtained for a typical van der Waals system described, e.g., by a Lennard-Jones potential. One obtains $\delta_{\rm re-entry} = 0.30$ and 0.117 for the HCY and SWS, respectively. It should be noted that the transition curve shown for $\delta = 0.30$ terminates at the spinodal line defined by the divergence of $S_q$ for $q = 0$. Beyond this point, MCT equations are meaningless and calculations of density correlators cannot be performed there within that theory.

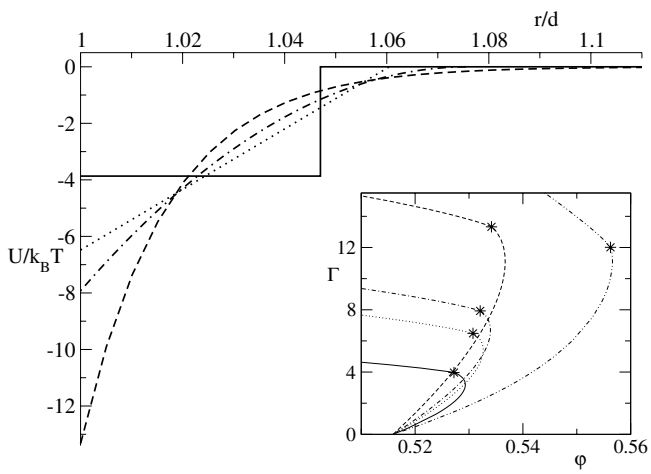


**Figure 2.** Attractive potentials $U$ relative to the thermal energy $k_B T$ as a function of the interparticle distance $r$ relative to the hard-sphere diameter $d$ for control parameters $V^*$ at the respective $A_4$-singularity. The curves refer to the SWS (——), TRI (· · · · · ·), AOS (— · —), HCY (– – –), and SHS (— · · —). The inset shows the cuts of the bifurcation surfaces through $\boldsymbol{V}^*$ for fixed attraction-range parameter $\delta = \delta^*$.

Figure 2 exhibits the four regular attraction potentials defined in equations (3) and (4) for control parameters at the respective $A_4$-singularities. The inset shows cuts through the liquid–glass transition surfaces for fixed range parameter $\delta^*$. The regular potentials are rather close to each other for $1.01 \leqslant r/d \leqslant 1.05$. The volume of the shell $1.00 < r/d < 1.02$ is smaller than that for the shell $1.02 < r/d < 1.04$. Within the latter, the attraction strength decreases in the sequence SWS, TRI, AOS, HCY. Therefore, the critical packing fraction $\varphi^*$ for the onset of an iso-structural glass transition increases in this sequence. One finds $\varphi^* = 0.5272$, 0.5307, 0.5321, and 0.5342, respectively. For the same reason, the maximum packing fraction of the liquid increases in this sequence. One gets $\varphi^{\max} = 0.5293$, 0.5326, 0.5340, and 0.5367, respectively. For Baxter's model, all mode-coupling effects have been cut off for $q > \pi d/\delta^*$. Therefore, the bonding effects are reduced compared to those for the regular potentials, and the values $\varphi^* = 0.5562$ and $\varphi^{\max} = 0.5566$ for the SHS are larger than the corresponding values for the regular potentials. Evaluating the structure factor of the SWS up to next-to-leading order as done in [11], one gets $\varphi^* = 0.5277$ and $\varphi^{\max} = 0.5299$. Indeed, the difference of these numbers from those calculated with the formulae from the appendix is small.

Structure factors $S_q$ at the $A_4$-singularities and the corresponding critical Debye–Waller factors $f_q^c$ are compared in figure 3. Also compared are the so-called critical amplitudes $h_q$. These are evaluated by a straightforward but involved procedure from the mode-coupling functional at the bifurcation point [1]. They quantify the susceptibility of the arrested structure. The increase of $(f_q - f_q^c)$ upon increasing $\boldsymbol{V} - \boldsymbol{V}^*$ is proportional to $h_q$ and so is the prefactor in the logarithmic decay laws that are the characteristic feature of the dynamics near a higher-order singularity [16]. The $S_q$ for various models mainly differ by a small shift parallel to the $q$-axis only. This shift reflects the decrease of the interparticle distance caused by the increase of $\varphi^*$. The $f_q^c$ oscillate in phase with $S_q$ and the $h_q$ oscillate in opposite phase, as known and explained for the simple HSS [1]. However, the $f_q^c$ are considerably larger and the $h_q$ are smaller than the corresponding quantities at the hard-sphere transition. This is a manifestation of the fact that the attractive part of the potential enforces localization, provided

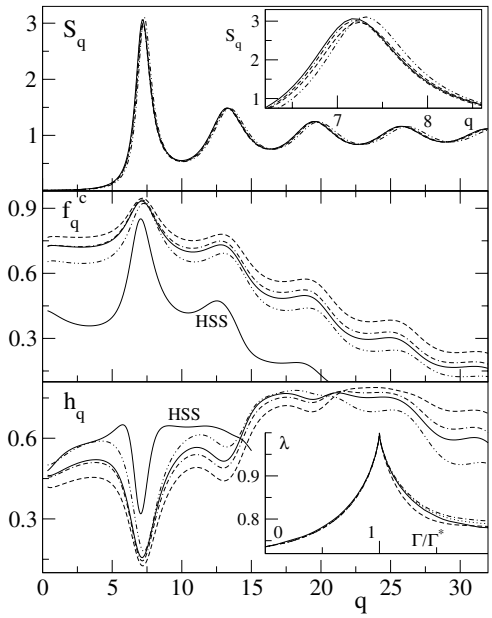


**Figure 3.** The structure factor $S_q$, critical Debye–Waller factor $f_q^c$, and critical amplitude $h_q$ for control parameters specifying the $A_4$-singularity $V^*$, SWS (——), HCY (– – –), and SHS (— · · —). The fourth curve (– – · – – ·) shows the results for the SWS using the structure factor up to next-to-leading order in $\delta$ [11]. The curves denoted by the HSS exhibit $f_q^c$ and $h_q$ for the critical point of the HSS. The inset from the lower panel shows the variation of the exponent parameter $\lambda$ along the liquid–glass transition curves through $\boldsymbol{V}^*$ from figure 2.

that a glass state is established. Within the wavevector region around the first diffraction peak, say $1 \leqslant qd \leqslant 10$, the Debye–Waller factor of the SWS differs from that of the HCY up to about 7% while this difference is minimal at the peak. The corresponding difference for the critical amplitude is about 9% which is maximal at the peak. The inset for the lowest panel of figure 3 displays the variation of the exponent parameter $\lambda$ for the liquid–glass transitions on the cuts $\delta = \delta^*$. Rescaled as a function of $\Gamma/\Gamma^*$, the $\lambda$ cannot be distinguished on the branch $\Gamma/\Gamma^* < 1$ dealing with transitions to the repulsion-dominated glass. On the branch $\Gamma/\Gamma^* > 1$, which deals with transitions to the attraction-dominated glass, the $\lambda$ for the various models are still very close to each other.

Figure 3 also exhibits results for the SWS evaluated with the structure factor in next-to-leading order of [11] in comparison with those based on the leading-order theory explained in appendix. Obviously the difference is too small to be of interest.

The macroscopic mechanical stiffness of liquids and glasses is quantified by the elastic moduli. The longitudinal modulus $M_{\mathrm{L}}$ specifies the stiffness for compressions and the transverse one $M_{\mathrm{T}}$, also called shear modulus $G'$, the stiffness for shear deformations. They are defined as constants of proportionality in the linearized stress–strain relation. In systems with Newtonian microscopic dynamics, they determine the speed of longitudinal and transverse sound, respectively, via $v_{\mathrm{L,T}} = \sqrt{M_{\mathrm{L,T}}/(\rho m)}$ with $\rho m$ denoting the mass density. For an ergodic system, the shear modulus vanishes, $M_{\mathrm{T}}^0 = 0$. The longitudinal modulus reads $M_{\mathrm{L}}^0 = \rho(k_{\mathrm{B}}T)S_0^{-1}$ with $S_0 = \lim_{q\to 0} S_q$. In the glass state, the moduli are larger: $M_{\mathrm{L,T}} = M_{\mathrm{L,T}}^0 + \delta M_{\mathrm{L,T}}$. The additional contributions are the positive long-time limits of

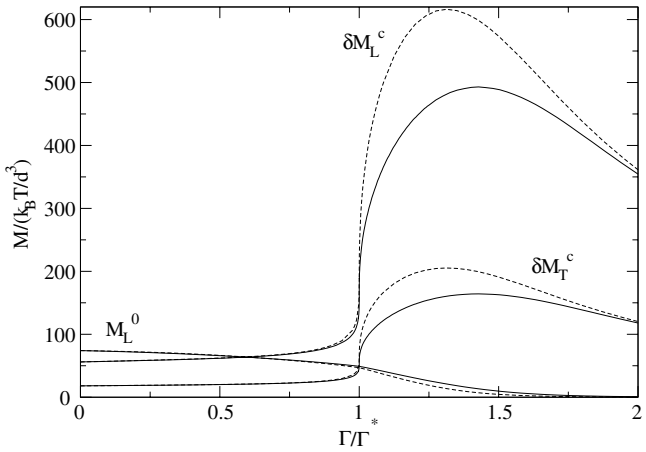


**Figure 4.** Longitudinal elastic moduli $M_{\mathrm{L}}$ and transverse elastic moduli $M_{\mathrm{T}}$ for the $\delta = \delta^*$ transition curve of the SWS (HCY) shown as full (dashed) curves. For the SWS, the structure factor from [11] was used. In the limiting case of the HSS, $M_{\mathrm{L}}^0 = 74.1$, $\delta M_{\mathrm{T}} = 18.1$, $\delta M_{\mathrm{L}} = 56.1$. At the $A_4$-singularity for the SWS (HCY), $\delta M_{\mathrm{T}}^* = 54.3$ (64.4), $\delta M_{\mathrm{L}}^* = 163.4$ (193.6). At the maximum $\delta M_{\mathrm{T}} = 164.2$ (205.3), $\delta M_{\mathrm{L}} = 493.0$ (616.3).

fluctuating-force correlators. For the latter, MCT yields [1]

$$\delta M_{\mathrm{L,T}} = \rho(k_{\mathrm{B}}T) \lim_{q\to 0} \sum_{\vec{k}+\vec{p}=\vec{q}} S_k S_p f_k f_p \{[\vec{k}c_k + \vec{p}c_p] \cdot \vec{e}_{\vec{q}}^{\,\mathrm{L,T}}\}^2 (\rho/2q^2). \tag{5}$$

Here $\vec{e}_{\vec{q}}^{\,\mathrm{L,T}}$ are unit vectors parallel and perpendicular to $\vec{q}$, respectively. The limit leads to

$$\delta M_{\mathrm{L,T}} = \rho(k_{\mathrm{B}}T) \int_0^\infty \mathrm{d}k \, \{\rho[S_k f_k k/(2\pi)]^2 w_{\mathrm{L,T}}(k)\}, \tag{6a}$$

$$w_{\mathrm{L}}(k) = c_k^2 + \tfrac{2}{3}(kc_k')c_k + \tfrac{1}{5}(kc_k')^2, \tag{6b}$$

$$w_{\mathrm{T}}(k) = \tfrac{1}{15}(kc_k')^2. \tag{6c}$$

In figure 4 the moduli for the SWS are compared with those for the HCY. The states are chosen on the cuts $\delta = \delta^*$ through the respective transition surface. The compression modulus $M^0$ of the liquid varies smoothly throughout, reflecting the well known increase of the compressibility with increasing attraction forces. The large variations of $\delta M_{\mathrm{L,T}}$ reflect the strong effect of bonding potentials on restoring forces [4, 11]. The same bonds are resisting shear as well as compression deformations. Therefore, there is no great difference in behaviour between the two moduli. The contributions to $\delta M_{\mathrm{L}}$ due to the first two terms in equation (6*b*) are smaller than the one due to the last term. Further, incidentally, these two contributions nearly cancel. Therefore, $\delta M_{\mathrm{L}}^{\mathrm{c}}$ differs from $3\,\delta M_{\mathrm{T}}^{\mathrm{c}}$ by less than 3% for $\Gamma < \Gamma^*$ and less than 0.5% for $\Gamma \geqslant \Gamma^*$. The universal properties of the $A_4$-bifurcation imply the following: the moduli vary smoothly for all $\Gamma \neq \Gamma^*$ and at the $A_4$-singularity there is a cubic-root singularity: $M(\Gamma) - M(\Gamma^*) \propto (\Gamma - \Gamma^*)^{1/3}$. The singular increase of $M$ with $\Gamma$ increasing through $\Gamma^*$ is a precursor of the discontinuous increase of $M$ upon crossing the glass–glass transition line for $\delta < \delta^*$. If $\Gamma$ increases further, the moduli have to decrease since the density decreases towards zero. Therefore, the moduli exhibit a maximum at some value of $\Gamma$ exceeding $\Gamma^*$. By continuity, such maximum also occurs for cuts with $\delta$ close but not equal to $\delta^*$, as was noticed before for the shear modulus [4, 17].

The clearest quantity for demonstrating the change of the glassification mechanism upon increasing the attraction is the variation of the particle's localization length $r_{\mathrm{s}}$ as a function

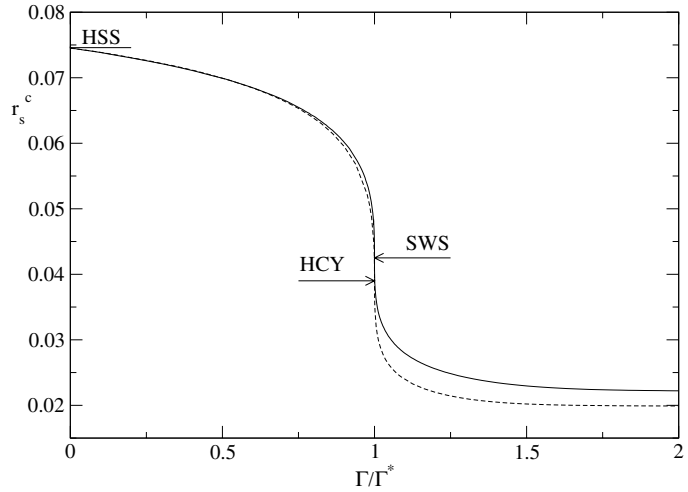


**Figure 5.** The localization length $r_s^c$ of a tagged particle for states on the $\delta = \delta^*$ transition curve for the SWS (HCY) shown as full (dashed) curve. At the $A_4$-singularity one gets $r_s^c/d = 0.0425$ (0.0390) as indicated by the arrows. The line labelled HSS marks the localization length $r_s^c/d = 0.0746$ for the HSS.

of $\Gamma$ for states on the cut $\delta = \delta^*$ (figure 5). This length is given by the mean-squared radius of a particle's long-time probability density. The Fourier transform of the latter is the Lamb–Mößbauer factor $f_q^s$ that is evaluated from an equation similar to equation (1) [1]. One ends up with an equation for the inverse of $r_s^2$ analogous to the equations for the moduli:

$$1/r_s^2 = \tfrac{1}{6}\int_0^\infty \mathrm{d}k\,\{\rho S_k f_k f_k^s [c_k k^2/\pi]^2\}. \tag{7}$$

With increasing $\Gamma$, $r_s^c$ decreases monotonically from the value for the HSS, $r_s^c/d = 0.0746$. The variation is smooth except for the cubic-root singularity at $\Gamma = \Gamma^*$. For strong bonding, $r_s^c$ decreases to a $\Gamma$-insensitive value of the order of the attraction potential range, as noted before for $\delta > \delta^*$ in the HCY [4].

## 3. Discussion

The first peculiarity of structural relaxation in systems of particles interacting with hard-sphere-like repulsions complemented by the short-ranged attractions predicted by MCT [3, 4], namely the re-entry phenomenon for the liquid–glass transition diagram, has been established recently [5–9]. This justifies focusing now on the more difficult task of testing the second prediction concerning the existence of $A_3$- and $A_4$-singularities. The signature of such higher-order singularities is the extreme stretching of relaxation curves, as has been explained on the basis of asymptotic expansions in terms of powers of logarithms in time [16]. The recent simulation results [7, 9] provide hints that there are such logarithmic decay laws. However, a more detailed analysis of the data would be required if one intended to arrive at compelling conclusions. The transition diagram exhibiting $A_3$-singularities is organized around an $A_4$-singularity. So far, such a singularity has been identified within a microscopic theory only for the SWS [11]. For this system, all parameters and amplitudes necessary for a discussion of the logarithmic decay laws have been evaluated [18]. In the present paper, $A_4$-singularities have been identified and characterized for a series of other attraction potentials in order to provide

some information on the sensitivity of the MCT results to the microscopic details assumed for the interaction.

The critical packing fractions $\varphi^*$ found for the $A_4$-singularities of the four regular potentials considered (figure 2) or the related largest values for the liquid packing $\varphi^{\max}$ exceed the critical packing fraction $\varphi^{\rm c}_{\rm HSS}$ of the HSS by about 3%. But the difference between these values for different models is about 1.4% only. It is not clear whether or not experiments can discriminate between the $\varphi^*$ or $\varphi^{\max}$ predicted for, say, the SWS and HCY. But simulation studies for the diffusivity of the kind published recently [8, 9] should be able to test our prediction $\varphi^{\max}_{\rm HCY} > \varphi^{\max}_{\rm SWS}$.

The singular potential for SHS was introduced by Baxter [10] as a certain attraction-range-to-zero limit in order to simplify equations from a mathematical point of view. But, within MCT, these simplifications cannot be made use of since the limit to zero for the range parameter $\delta$ must not be permuted with the limit to infinity for the wavevectors in the mode-coupling integrals. The problem can be handled by introducing some wavevector cut-off [3, 4]. This is equivalent to introducing a regular potential leading to a considerably larger $\varphi^* - \varphi^{\rm c}_{\rm HSS}$ than found for the other potentials examined above.

It is well known that the structure factor theories used in this paper lead to unsatisfactory results for the thermodynamic functions. Great progress has been made to improve on this, as is discussed, e.g., in [14]. The thermodynamic functions are derived from the zero-wavevector limits of correlators. However, in contrast to the limit of large wavevectors, which is important for capturing the essential physics of the glass transition, small-$q$ effects play a minor role for the transition curves. As already demonstrated for the SWS in [11], artificially setting the structure factor input to zero for $qd < 4$ does not alter the transitions qualitatively. For $\Gamma \gtrapprox \Gamma^*$ where large-$q$ values dominate, transition lines are in accordance even quantitatively.

The differences among the structure factors of the various models for wavevectors accessible in scattering experiments for colloids, say $2 \leqslant qd \leqslant 15$, are very small if the states at the $A_4$-singularity are compared (figure 3). However, the differences between the Debye–Waller factors and the critical amplitudes are of the order of 5%. The $f^{\rm c}_q$ and $h_q$ determine the amplitudes of the leading-order formulae for the intermediate-scattering functions for states near an $A_4$-singularity in a similar manner to how they determine the corresponding results near an liquid–glass $A_2$-transition [16]. If they could be deduced from a data analysis with similar accuracy to what one can achieve for data near an $A_2$-singularity, one could discriminate, e.g., between the square-well model and the HCY.

The tagged particle localization is described by the Lamb–Mößbauer factor, $f^{\rm s}_q$, that can be measured by means of incoherent scattering. It is a bell-shaped function of $q$ and its width can be quantified by the localization length $r_{\rm s}$: $f^{\rm s}_q = 1 - (qr_{\rm s})^2 + \mathcal{O}(q^4)$. As expected from the shape of the attractive potentials at the $A_4$-singularity (figure 2), $r^*_{\rm s}$ is smaller for the HCY than for the SWS by 10%. The MCT brings it out that $r^{\rm c}_{\rm s}$ becomes insensitive to $\Gamma$ for strong attraction. For the SWS (HCY) one gets $r^{\rm c}_{\rm s}/d = 0.022$ (0.020) for $\Gamma/\Gamma^* > 1.8$ within 1% accuracy.

The largest difference between the SWS and HCY is found at the maximum of the elastic moduli where the HCY is about 20% stiffer than the SWS. Taking the critical moduli of the HSS as reference, the maxima of the SWS and HCY should be at 9 or 11 times that value, respectively, as shown in figure 4.

The line of glass–glass transitions occurring for the cuts through the bifurcation surface for $\delta < \delta^*$ has an analogue in the line of iso-structural phase transitions from one face-centred cubic crystal to another one with a different lattice constant, identified for systems similar to the ones discussed above [19–22]. Similar to what is shown in figure 1, the end-point of the phase-transition line for the HCY also exhibits a critical attraction constant $\Gamma^{\rm c}$ that increases

with decreasing range parameter $\delta$. However, the value $\Gamma^c$ for phase transitions of the SWS was found to be practically independent of $\delta$ [20]. In contrast to this finding for the crystal–crystal transition, the end-point of the glass–glass transition line of the SWS behaves quite similarly to that found for the HCY.

Summarizing, one can conclude that the MCT predictions for the dynamics near an $A_4$-singularity are rather robust. At the present state of discussion, one can use any of the models studied so far to predict data semiquantitatively. There are two reservations. First, the quality of the theories applied for the evaluation of the structure factors $S_q$ is not known for the high-density regime of interest. The $S_q$ are, however, the essential input functions for all quantitative considerations. Second, the range of validity of the basic MCT equations of motion are not understood—not even qualitatively. Quantitative results of MCT have been tested with encouraging outcomes for the HSS [23], binary Lennard-Jones systems [24], and silica [25]. It remains to be tested by experiment or computer simulation whether or not the theory can also describe the systems studied in this paper.

**Acknowledgments**

We thank J Bergenholtz, M Fuchs and Th Voigtmann for discussion and J Bergenholtz for assistance while implementing the HCY structure factor. Our work was supported by the DFG grant Go 154/13-1.

## Appendix A. Structure factors

For the calculation of the structure factors we use a scheme developed earlier for the SWS [11]. The short-ranged attraction of the potential from equation (4) added to the hard core is treated in the mean-spherical approximation and the resulting equations are expanded in the small parameter $\delta$. The structure factor is expressed in terms of Baxter's factor function $Q(r)$ [26]:

$$S_q^{-1} = \hat{Q}(q)\hat{Q}(q)^*, \tag{A.1}$$

$$\hat{Q}(q) = 1 - 2\pi\rho \int_0^\infty \mathrm{d}r \exp[\mathrm{i}qr]Q(r). \tag{A.2}$$

In the leading-order approximation, one gets a shifted parabola within the hard core, $0 \leqslant r \leqslant 1$:

$$Q(r) = \frac{a}{2}(r^2 - 1) + b(r - 1) + \frac{K}{n}, \tag{A.3}$$

and a polynomial within the attraction shell, $1 \leqslant r \leqslant 1 + \delta$:

$$Q(r) = \frac{K}{n}\left(\frac{1 + \delta - r}{\delta}\right)^n, \qquad 1 \leqslant r \leqslant 1 + \delta. \tag{A.4}$$

Here, the hard-core diameter $d$ is used as the unit of length. For $r > 1 + \delta$, the factor function is zero. The various constants are given in concise forms, using $K = \Gamma\delta$, as

$$a = \frac{1 + 2\varphi}{(1 - \varphi)^2} - \frac{12\varphi}{(1 - \varphi)}\frac{K}{n}, \qquad b = \frac{-3\varphi}{2(1 - \varphi)^2} + \frac{6\varphi}{(1 - \varphi)}\frac{K}{n}. \tag{A.5}$$

Taking the limit $\delta \to 0$ can be carried out in equations (A.3)–(A.5) in the sense of [10]. This yields the result for $S_q$ used in [3, 4]. However, this procedure appears unjustified. Within the mode-coupling functional, equation (1*b*), one needs values of $S_q$ also for large wavevectors. But the limits $q \to \infty$ and $\delta \to 0$ cannot be permuted. Introduction of the cut-off is one way to redefine the model so that the MCT remains meaningful. A more appealing procedure is to consider the $\delta$-expansion from [11] and define as Baxter limit the one where terms of order

$\delta^1$ are neglected compared to those of order $\delta^0$. But this is just the approximation defined by equations (A.3)–(A.5) that was used in this paper. It is in no respect more complicated to handle than the approximation proposed originally [10].

## References


[1] Götze W 1991 Aspects of structural glass transitions *Liquids, Freezing and Glass Transition (Les Houches Summer Schools of Theoretical Physics Session LI (1989))* ed J-P Hansen, D Levesque and J Zinn-Justin (Amsterdam: North-Holland) pp 287–503

[2] Arnol'd V I 1992 *Catastrophe Theory* 3rd edn (Berlin: Springer)

[3] Fabbian L, Götze W, Sciortino F, Tartaglia P and Thiery F 1999 *Phys. Rev.* E **59** R1347–50
Fabbian L, Götze W, Sciortino F, Tartaglia P and Thiery F 2000 *Phys. Rev.* E **60** 2430

[4] Bergenholtz J and Fuchs M 1999 *Phys. Rev.* E **59** 5706–15

[5] Pham K N, Puertas A M, Bergenholtz J, Egelhaaf S U, Moussaïd A, Pusey P N, Schofield A B, Cates M E, Fuchs M and Poon W C K 2002 *Science* **296** 104–6

[6] Eckert T and Bartsch E 2002 *Phys. Rev. Lett.* **89** 125701

[7] Puertas A M, Fuchs M and Cates M E 2002 *Phys. Rev. Lett.* **88** 098301

[8] Foffi G, Dawson K A, Buldyrev S V, Sciortino F, Zaccarelli E and Tartaglia P 2002 *Phys. Rev.* E **65** 050802(R)

[9] Zaccarelli E, Foffi G, Dawson K A, Buldyrev S V, Sciortino F and Tartaglia P 2002 *Phys. Rev.* E **66** 041402

[10] Baxter R J 1968 *J. Chem. Phys.* **49** 2770–4

[11] Dawson K, Foffi G, Fuchs M, Götze W, Sciortino F, Sperl M, Tartaglia P, Voigtmann Th and Zaccarelli E 2001 *Phys. Rev.* E **63** 011401

[12] Cummings P T and Smith R R 1979 *Chem. Phys.* **42** 241–7

[13] Asakura S and Oosawa F 1958 *J. Polym. Sci.* **33** 183–92

[14] Foffi G, McCullagh G D, Lawlor A, Zaccarelli E, Dawson K A, Sciortino F, Tartaglia P, Pini D and Stell G 2002 *Phys. Rev.* E **65** 031407

[15] Dawson K A, Foffi G, McCullagh G D, Sciortino F, Tartaglia P and Zaccarelli E 2002 *J. Phys.: Condens. Matter* **14** 2223–35

[16] Götze W and Sperl M 2002 *Phys. Rev.* E **66** 011405

[17] Zaccarelli E, Foffi G, Dawson K A, Sciortino F and Tartaglia P 2000 *Phys. Rev.* E **63** 031501

[18] Sperl M 2003 in preparation

[19] Bolhuis P and Frenkel D 1994 *Phys. Rev. Lett.* **72** 2211–14

[20] Bolhuis P, Hagen M and Frenkel D 1994 *Phys. Rev.* E **50** 4880–90

[21] Tejero C F, Daanoun A, Lekkerkerker H N W and Baus M 1994 *Phys. Rev. Lett.* **73** 752–5

[22] Tejero C F, Daanoun A, Lekkerkerker H N W and Baus M 1995 *Phys. Rev.* E **51** 558–66

[23] van Megen W 1995 *Transp. Theory Stat. Phys.* **24** 1017–51

[24] Nauroth M and Kob W 1997 *Phys. Rev.* E **55** 657–67

[25] Sciortino F and Kob W 2001 *Phys. Rev. Lett.* **86** 648–51

[26] Hansen J-P and McDonald I R 1986 *Theory of Simple Liquids* 2nd edn (London: Academic)